Metallomics

Accepted Manuscript

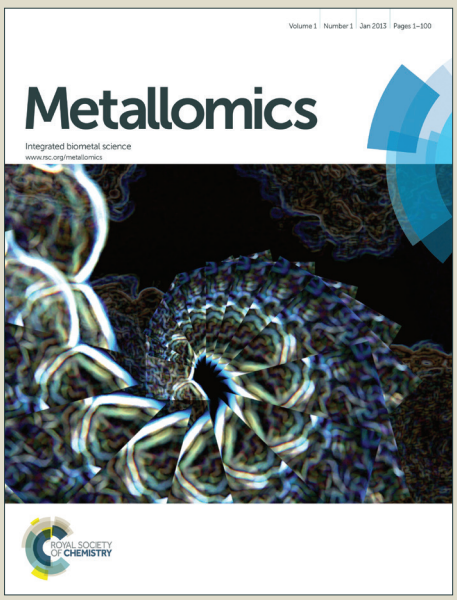

ROYAL SOCIETY OF CHEMISTRY

www.rsc.org/metallomics

A proteomic approach to investigate the effects of cadmium and lead on human primary renal cells

Eugenio Galano[1,2,°], Angela Arciello[1,2,°], Renata Piccoli[1,2], Daria Maria Monti[1,2,*] and Angela Amoresano[1,2]

[1]Department of of Chemical Sciences, University of Naples "Federico II", Italy

[2]National Institute of Biostructures and Biosystems (INBB), Rome, Italy.

° These authors equally contributed to the paper

*Correspondance: Dr Daria Maria Monti, Department of Chemical Sciences, University of Napoli "Federico II", Monte Sant'Angelo, via Cinthia 4, 80126, Naples, Italy.

Email: mdmonti@unina.it Phone: +39 081 679150

Keywords: Heavy metals, proteomics, cytotoxicity

Abbreviations

HRCE, Human Renal Cortical Epithelial cells

ICP-MS, Inductively Coupled Plasma-MS

nanoLC-MS/MS, nano Liquid Chromatography tandem Mass Spectrometry

GAPDH: glyceraldheyde 3-phosphate dehydrogenase

SapK: stress-activated MAP kinase

Abstract

Heavy metals are strongly poisonous for the environment, but their impact on living cells and organisms is poorly understood at a molecular level. We investigated the effects of cadmium and lead on the viability of primary HRCE cells. A severe dose- and time-dependent inhibition of cell viability was induced by either heavy metals. Cell mortality was due to apoptotic death, as demonstrated by a decrease of procaspase-9 and down-regulation of the anti-apoptotic marker Bcl-2 with consequent activation of caspase-3. By ICP-MS analyses we determined the amount of heavy metals in the intracellular compartment, which was found to be higher for lead than cadmium. To gain insights on the effects of heavy metals on cell proteome, a systematic investigation was performed, based on 2D-PAGE, image analysis, protein identification and bioinformatics analyses. Among more than 300 protein spots visualized by bidimensional maps, 27 proteins were found to be altered in their expression levels following heavy metal exposure. These proteins were all identified by nanoLC-MS/MS. The majority of them was found to be involved in apoptotic pathways, protein folding or energetic metabolism, which eventually lead to cell death. Taking advantage of an integrated workflow, we identified specific protein targets of heavy metals, which represent a contribution to the identification of potential biomarkers of heavy metal environmental pollution.

1. Introduction

Copper, lead, manganese, cadmium, molybdenum, mercury, arsenic, often referred to as "heavy metals", are poisonous for natural world, animals and humans[1]. Among the heavy metals, some actively participate to biological processes. This is the case of iron, cobalt, copper, manganese, molybdenum and zinc. Other metals, such as lead, cadmium, mercury and arsenic, not involved in biological functions, are harmful even at very low concentrations. Actually, being the exposure to these metals the primary cause of work related diseases, they have been extensively considered and their effects on human health monitored and controlled by international organizations[2]. Nowadays, environment, food and water are often contaminated by a range of chemicals and heavy metals, such as lead, cadmium, arsenic, chromium and mercury, with a consequent deep impact on human health. Different are the ways of heavy metals intake. Smoking is a major source of cadmium exposure; exposition to mercury takes place via food, fish being a major source. Air, food and drinking water are the main via of population intake of lead and arsenic[3]. Nevertheless, despite remediation procedures, heavy metal exposure and contamination still remains a challenging task[4].

Many studies have confirmed that heavy metals activate signaling pathways and carcinogenic effects of metals have been mainly related to the activation of redox-sensitive transcription factors. As discussed by Valko and coworkers[5], iron, copper, chromium, vanadium and cobalt undergo redox-cycling reactions. On the other hand, mercury, cadmium and nickel toxicity are involved in glutathione depletion and binding to protein sulfhydryl groups. Free divalent Cd and Pb cations also bind to protein sulfhydryl groups affecting protein structure and function; furthermore, they may also affect enzymatic reactions in which calcium plays a role.

Disruption of metal ions homeostasis in a cell may lead to oxidative stress, increased lipid peroxidation, protein modification and other effects, all symptomatic for numerous diseases,

involving cancer, cardiovascular diseases, diabetes, atherosclerosis, neurological disorders (Alzheimer's disease, Parkinson's disease), chronic inflammation and others[6]. Because of their ability to reabsorb and accumulate divalent metals, kidneys are the first target organs of heavy metal toxicity[7]. Cadmium and lead toxicity may cause nephropathies even at low doses, especially in the case of cadmium. It has also been demonstrated that cadmium induces apoptosis in human embryonic cells (HEK 293), both through caspase-independent and -dependent pathways that involve mitochondria[8]. Moreover, it has been reported that cadmium induces apoptosis also in human hepatocellular carcinoma cell lines (HepG2 and PLC/PRF/5) in a time- and concentration-dependent manner[9]. In particular, it was well demonstrated that lead and cadmium have a direct effect on the kidneys, being particularly nephrotoxic even at physiological levels[10]. However, the molecular mechanism at the basis of cadmium and lead toxicity, recognized as environmental toxicants and carcinogens, is still unknown, even if many efforts have been applied so far using different analytical procedures. Jeon and coworkers[11] identified by a proteomic approach proteins involved in the adaptive responses to cadmium in U937 cells. More recently, a comparative proteomic analysis between a zinc- and cadmium-resistant human epithelial cell line (HZR, high zinc-resistant HeLa cells) and parental HeLa cells has been carried out[12].

Here, a proteomic approach, based on 2D-PAGE, image analysis and protein identification by nanoLC-MS/MS, was employed to define the toxic effect and alterations in protein levels caused by exposure of primary human renal cortical epithelial (HRCE) cells to cadmium or lead, in order to gain insights at a molecular level on cellular responses. ICP-MS analyses were also performed to establish the presence of heavy metals in the intracellular compartment and to determine their amount after 24 h exposure. A comparison of the proteomes of treated versus untreated cells provided a list of proteins significantly altered in their expression levels by heavy

metals exposure (Cd or Pb). To the best of our knowledge, for the first time an integrated workflow, based on bioinformatics analysis, Western blotting and fluorescence analytical tools, was exploited revealing that cadmium and lead induce proteome alteration and activate apoptotic cell death.

2. Material and Methods

2.1 Materials

Trypsin, DTT, iodoacetamide, puromycin and α-cyano-4-hydroxycinnamic acid were purchased from Sigma-Aldrich. The chemiluminescence detection system (SuperSignal® West Pico) was from Pierce. HRCE cells (Innoprot) were cultured in basal medium, supplemented with 2% foetal bovine serum, epithelial cell growth supplement and antibiotics, all from Innoprot, in a 5% CO_2 humidified atmosphere at 37ºC. Antibodies were purchased from Cell Signal Technology.

2.2 Analysis of apoptotic pathway

Cells were plated at a density of 2×10^4 cells/cm^2 in complete medium for 24 h and then treated for 24 and 48 h with 10 µg/mL $CdCl_2$ or with 100 µg/mL $PbCl_2$. At the end of incubation, both untreated and treated cells were analyzed. To prepare cell lysates, HRCE cells were scraped off in phosphate buffer, centrifuged at 1,000 g for 10 min and resuspended in lysis buffer (1% NP-40 in PBS, pH 7.4) containing protease inhibitors. After 30 min incubation on ice, lysates were centrifuged at 14,000 g for 30 min at 4°C. Upon determination of total protein concentration in the supernatant by the Bradford assay, samples were analyzed by SDS-PAGE and Western blotting using specific antibodies directed towards apoptotic markers (procaspase-3, procaspase-9, Bcl-2, phospho-SapK). To normalize to internal standard signals, antibodies against alpha-actin and GAPDH were used. To detect apoptotic nuclei, cells were seeded on glass coverslips in 24-well plates and grown to semi-confluency. Cells were incubated for 24 and 48 h with $CdCl_2$ (10 µg/mL) or $PbCl_2$ (100 µg/mL) in complete medium, after which nuclei were stained with 1 µg/mL Hoechst 33342 for 10 min at 37°C. Cells were then washed with PBS, fixed for 10 min at RT with 2% paraformaldehyde in PBS and mounted in 50% glycerol

in PBS. In a parallel experiment, cells were treated with puromycin (10 μg/mL) for 4 h as a control of apoptotic death. Samples were examined using a Leica 6000 UV microscope and a Leica TCS SP5 confocal microscope, equipped with a Leica application suite software. All images were taken under identical conditions.

2.3 ICP-MS analysis

Cells were plated and treated with $CdCl_2$ (10 μg/mL) or with $PbCl_2$ (100 μg/mL) as described above and, after 24 h, the medium of treated and untreated cells was withdrawn and cells were extensively washed with PBS. Metal content was determined by ICP-MS analyses. The total metal amount was calculated by analyzing unconditioned medium supplemented with 10 μg/mL $CdCl_2$ or with 100 μg/mL $PbCl_2$. The amount of extracellular metals was obtained by the sum of the metal content of the conditioned medium and PBS wash, while the intracellular amount was measured by analyzing the cellular content. In particular, the cell pellet (1.9 and 1.2×10^6 cells for untreated and treated cells, respectively) was resuspended in 1 mL Milli-Q water, transferred in a Teflon vessel and treated with 6 mL HNO_3 (67-69% ultrapure) and 2 mL 30% H_2O_2 in a microwave oven (Milestone Ethos 900-Mega II). Mineralization was achieved with the following microwave oven program: 20 min to reach 220°C at 1400 W; 15 min at 220°C and 1400 W; ventilation for 30 min. The solution was then transferred into polystyrene liners, an aliquot of each sample was diluted 1:10 (v/v) with Milli-Q water and finally analyzed with an Agilent 7700 ICP-MS from Agilent Technologies, equipped with a frequency-matching RF generator and 3rd generation Octopole Reaction System (ORS^3), operating with helium gas in ORF. The following parameters were used: radiofrequency power 1550 W, plasma gas flow 14 L/min; carrier gas flow 0.99 L/min; He gas flow 4.3 mL/min. ^{103}Rh was used as an internal standard (50

μg/L final concentration). Multi-element calibration standards were prepared in 5% HNO_3 at 4 different concentrations (1, 10, 50, and 100 μg/L).

2.4 Cytotoxicity assays

Cells were seeded in 96-well plates (100 μL/well) at a density of 5×10^3/well. Heavy metals to be tested were added to the cells 24 h after seeding for time- and dose-dependent cytotoxic assays. At the end of incubation, cell viability was assessed by the MTT assay. MTT reagent, dissolved in DMEM in the absence of phenol red (Sigma-Aldrich), was added to the cells (100 μL/well) to a final concentration of 0.5 mg/mL. Following 4 h incubation at 37°C, the culture medium was removed and the resulting formazan salts were dissolved by adding isopropanol containing 0.1 N HCl (100 μL/well). Absorbance values of blue formazan were determined at 570 nm using an automatic plate reader (Microbeta Wallac 1420, Perkin Elmer). Cell survival was expressed as percentage of viable cells in the presence of the heavy metal under test, with respect to control cells grown in the absence of metal. The IC_{50} value was the metal concentration determining 50% inhibition of cell viability with respect to untreated cells.

2.5 2D-PAGE

The first dimensional electrophoresis was carried out on non-linear wide-range immobilized pH gradients (pH 4-7; 7 cm long IPG strips; GE Healthcare) and achieved using the Ettan IPGphor system (GE Healthcare). 200 μg of protein extracts were precipitated with methanol/chloroform according to Wessel[13] and solubilized in 125 μL of rehydratation buffer and 0.2% (v/v) carrier ampholyte for 12 h, at 50 mA, at 20°C. The strips were then focused according to the following electrical conditions at 20°C: 500 V for 30 min, 1,000 V for 30 min, 5,000 V for 10 h, until a total of 15,000 V was reached. After focusing, analytical and preparative IPG strips were

equilibrated for 15 min in 6 M urea, 30% (v/v) glycerol, 2% (w/v) SDS, 0.05 M Tris-HCl, pH 6.8, 1% (w/v) DTT, and subsequently for 15 min in the same urea/SDS/Tris buffer solution but substituting the 1% (w/v) DTT with 2.5% (w/v) iodoacetamide. The second dimension was carried out on 12.5% (w/w) polyacrylamide gels (10×8cm×1mm) at 25 mA/gel constant current and 10°C until the dye front reached the bottom of the gel, according to Laemmli[14] and Hochstrasser[15]. MS-preparative gels were stained overnight with colloidal Coomassie Brilliant Blue and destained with MilliQ grade water.

2.6 Image analysis

Gel images were acquired with an Epson expression 1680 PRO scanner. Computer-aided 2-D image analysis was carried out using the ImageMasterTM 2D Platinum software. Relative spot volumes (%v) (v = integration of OD over the spot area; %v = v single spot/v total spot) were used for quantitative analysis in order to decrease experimental errors. The normalized intensity of spots on three replicate 2-D gels was averaged and standard deviation was calculated for each condition. A few initial reference points were affixed for gels alignment, the first step of the images analysis. Landmarks are positions in one gel that correspond to the same position in the other gels. Then, the software automatically detects spots, which represent the proteins on the gels. The software "matches" the gels and the corresponding spots which are paired. The pair is the association between spots that represent the same protein in different gels. Pairs are automatically determined using ImageMaster powerful gel matching algorithm. The pairs were also evaluated by 3-D spots view. Differences in spot intensity between the gels are identified by relative quantification; spots that exhibit a variation of ± 20% were considered not affected by metals exposure.

2.7 Peptide analysis and protein identification

Spots selected by image analysis were excised from the gels and destained by repetitive alternate washes with 0.1 M NH_4HCO_3, pH 7.5 and ACN. Enzymatic digestion was carried out with 100 ng of trypsin in 50 µL of 10 mM NH_4HCO_3 buffer, pH 7.8. Gel pieces were incubated at 37°C overnight. Peptides were then extracted by washing the gel particles with 10 mM NH_4HCO_3 and 1% formic acid in 50% ACN at room temperature. The resulting peptide mixtures were filtrated using 0.22 PVDF filter from Millipore. The peptide mixtures were analysed by nanoLC-chip MS/MS**,** using a CHIP MS 6520 QTOF equipped with a capillary 1200 HPLC system and a chip cube (Agilent Technologies). After loading, the peptide mixture (8 µL in 0.1% formic acid) was first concentrated and washed at 4 µL/min in 40 nL enrichment column (Agilent Technologies chip), with 0.1% formic acid in 2% ACN as eluent. The sample was then fractionated on a C18 reverse-phase capillary column (75 µm × 43 mm in the Agilent Technologies chip) at flow rate of 400 nL/min with a linear gradient of eluent B (0.1% formic acid in 95% ACN) in A (0.1% formic acid in 2% ACN) from 7 to 60 % in 50 min. Eluted peptides were ionized to charge states 1+, 2+ or higher by the electrospray source. Doubly and triply charged peptides were selected and analyzed using data-dependent acquisition of one MS scan (mass range from 400 to 2,000 m/z) followed by MS/MS scans of the three most abundant ions in each MS scan. Collision energy (CE) applied during peptide fragmentation is calculated by the sequent empirical equations: CE= 4V/100Da -2,4V. Raw data from nanoLC–MS/MS were analyzed and converted in mzData (.XML) file format using Qualitative Analysis software (Agilent MassHunter Workstation Software, version B.02.00) and MS/MS spectra were searched against non-redundant protein databases UniprotSprot (Sprot_40.21.fasta, 533049 sequences; 189064225 residues), with the taxonomy restriction to *Homo sapiens* (20252 sequences), using in house MASCOT software (www.matrixscience.com) version: 2.1.04. The Mascot search parameters

were: “trypsin” as enzyme allowing up to 3 missed cleavages, carbamidomethyl on cysteine residues as fixed modification, oxidation of methionine and formation of pyroGlu N-term on glutamine were selected as variable modifications, 20 ppm MS/MS tolerance and 0.6 Da peptide tolerance. By data analysis, threshold provided to evaluate quality of matches for MS/MS data was found to be 25. No single peptide identification, even if unique, and peptide with a score lower than 25, were accepted.

2.8 Bioinformatic analysis

Differentially expressed proteins were listed and uploaded into IPA (Ingenuity Systems, www.ingenuity.com)[16], to highlight direct relationships between candidate proteins using networks and canonical pathways. Two sets of data were created, inferred to the protein identified after Cd(+2) and Pb(+2) exposure. Both sets of data, containing a list of protein IDs from UniprotK databases, were uploaded into IPA software online. Ingenuity Knowledge Base, the core behind IPA, provide a wide range of high-quality detailed information, including direct and indirect protein interaction networks, thus aiding generation of hypotheses for a comprehensive analysis of large number of data.

3. Results

3.1 Effects of heavy metals on cell viability

The effects of cadmium and lead on cell viability were analyzed by using a primary human cell line derived from kidney. The viability of cells treated for 24 h with increasing amounts of $CdCl_2$ or $PbCl_2$ was tested by the MTT reduction assay, as an indicator of metabolically active cells. In Fig. 1A and B, the results of dose-response experiments are shown. The values are the average of 3 independent experiments, each carried out with triplicate determinations. We observed a dose-dependent inhibition of cell viability associated to the treatment with either heavy metals, with cadmium the most effective. The IC_{50} value, i.e. the metal concentration determining 50% inhibition of cell viability with respect to untreated cells, was found to be 10 μg/mL for $CdCl_2$ and 100 μg/mL for $PbCl_2$. The results of time-course experiments are shown in Fig. 1C, where the experimental points represent the average of at least 3 independent experiments, each carried out with triplicate determinations. Cells were treated with $CdCl_2$ (10 μg/mL) or with $PbCl_2$ (100 μg/mL) for a length of time ranging from 2 to 72 h and then analyzed by MTT assays. In both cases we observed a time-dependent inhibition of cell viability. Cadmium was found to be significantly more effective than lead, considering that it was tested at a concentration 10 times lower. However, in dose-response experiments increasing cell mortality was observed reaching a maximum value at about 60 and 50%, respectively, which did not further increase even when higher doses of $CdCl_2$ or $PdCl_2$ were used. Similarly, in time-course experiments cell viability decreased to about 25% for both metals after 72 h incubation.

To investigate the cellular response to heavy metals, the metal amount able to induce 50% mortality (IC_{50}) was used. HRCE cells were incubated for 24 and 48 h with the heavy metals and stained with the fluorescent apoptotic marker Hoechst 33342, which binds to the highly condensed chromatin of apoptotic cell nuclei[17,18] (Fig. 2). Cells treated with puromycin, an

apoptosis inducing agent, were used as a positive control. Fluorescence microscopy images indicated that at 24 and 48 h the nuclei of Cd-treated cells were prominently stained with the dye, more evident at 48 h, and often appeared abnormal in shape (Fig. 2, right panels). In the case of Pb-treated cells, we observed that nuclei staining was evident only at 48 h, but less pronounced than in Cd-treated cells. Considering that $PbCl_2$ concentration tested was associated to 50% mortality, these results suggest that different death mechanisms might be activated, with apoptosis acting as a late event.

To test apoptosis induction by heavy metals, we analyzed different apoptotic markers activated along the pathway. Activation of stress-activated MAP kinase (SapK) has been shown to be an early event in apoptosis; when phosphorylated, SapK translocates to the mitochondria where it phosphorylates and inactivates anti-apoptotic Bcl-2 family members with consequent activation of caspase-9. The final event of this cascade leads to the activation of caspase-3, considered the executive enzyme of apoptotic cell death.

HRCE cells were treated with $CdCl_2$ (10 μg/mL) or with $PbCl_2$ (100 μg/mL) for 24 and 48 h. Cell lysates were then prepared and analysed by Western blotting using specific antibodies directed towards different apoptotic markers (procaspase-3, procaspase-9, Bcl-2, phospho-SapK), as reported in Table 1, followed by densitometric analyses. Endogenous alpha-actin or GAPDH were used as internal standards. In Fig. 3 the results of Western blot analyses after exposure to heavy metals are reported. In cells treated with $PbCl_2$ after 24 h (Fig. 3A), we did not observe activation of caspase-3 or SapK phosphorylation, whereas a modest decrease (15%) of procaspase-9 was observed, followed by a late decrease (48 h) of procaspase-3 (Fig. 3B). A significant decrease of Bcl-2 immunopositive signal was also observed.

Instead, in cells treated with $CdCl_2$ procaspase-9 was cleaved, as only 33% of the procaspase-9 signal was detectable upon metal treatment. A strong signal associated to phospho-SapK was

also observed after 24 h incubation (Fig. 3A). Activation of procaspase-3 was clearly observed at 48 h, not yet evident at 24 h (Fig. 3B). We also observed a decrease of Bcl-2 immunopositive signal.

These results indicate that both Cd(+2) and Pb(+2) down-regulate Bcl-2 and induce caspase-3 activation, with Cd(+2) being much more effective as a toxic agent.

3.2 Heavy metals quantification by ICP-MS

The multielemental analysis on different samples was performed by ICP-MS. The standard addition approach for calibration on 3 concentration levels was used in order to keep matrix induced variations under control. A minimum of three replicates of each calibration standard was run. Reagent blanks were run together with matrices.

After treatment with 10 µg/mL $CdCl_2$ or 100 µg/mL $PdCl_2$ for 24 h, the amount of metals recovered in the cell conditioned medium, as well as in the cell wash and cell lysate, was determined by ICP-MS (Table 2). The extracellular and intracellular amount of metals was calculated as described in the Methods section and expressed as percentage of the total amount determined. We found that low amounts of metals were internalized in the cells, as about 0.3% of Cd(+2) and 0.7% of Pb(+2) were detected in the cell lysate.

3.3 Proteomic analyses

Protein extracts from HRCE cells untreated (Fig. 4A), or exposed for 24 h to 10 µg/mL of $CdCl_2$ (Fig. 4B) or to 100 µg/mL of $PbCl_2$ (Fig. 4C), were fractionated by 2D-GE and stained with colloidal Coomassie Blue. Gels were run in triplicate and the bidimensional maps were compared using the ImageMaster 2D Platinum 6.0 software. All spots that exhibited a variation higher than 20% when compared to the control were considered significant. More than 300 most

relevant protein spots were visualized and compared (Fig. 4). Among these, 25 spots resulted to be significantly altered following exposure to heavy metals. Upon $PbCl_2$ treatment, nine protein spots showed an increased signal volume, whilst 13 displayed a significant decrease. As for cadmium exposure, 18 spots showed a decreased volume upon $CdCl_2$ treatment.

The 25 selected spots were excised from the gels, digested with trypsin and the resulting peptide mixtures were analyzed by nanoLC-MS/MS experiments. The peptide mixtures were fractionated by nanoHPLC and sequenced by MS/MS generating sequence information on individual peptides. MS/MS spectra were used to search for a non-redundant sequence against UniprotSprot databases using the in-house MASCOT software, taking advantage of the specificity of trypsin and of the taxonomic category of the samples. The number of measured masses matching within the given mass accuracy was recorded and the proteins showing the highest number of peptide matches were examined leading to the identification of the protein components. As further selection criteria, only the proteins identified by MASCOT search with at least 2 peptides with an individual ion score higher than 25 and found exclusively in the replicates were selected. The list of the 27 proteins identified by this approach is reported in Table 3. The data associated with protein identifications are reported in supplementary material (Table S1).

As shown in Table 3, most of the proteins were affected by both metals, whereas some were influenced either by lead or cadmium. Upon lead exposure, some proteins were found to be up-regulated and others down-regulated, whereas following cadmium exposure all the affected ones were down-regulated. Among these, some resulted undetectable being under the staining detection limit.

On the basis of literature information, the identified proteins were classified into functional groups, generating a sets of data for each metal, as shown in Fig. 5A and B relative to Pb(+2) and

Cd(+2) exposure, respectively. The majority of the proteins, whose levels were significantly affected by the exposure to Cd(+2) or Pb(+2), resulted to be involved in specific functions, such as apoptotic pathways, energetic metabolism and protein folding. This is particularly true for cadmium treatment, as about 50% of the identified proteins were implicated in apoptosis. Other altered proteins were found to be involved in protein synthesis and cytoskeleton formation.

3.4 IPA canonical network

Differentially expressed proteins were listed and uploaded into IPA (Ingenuity Systems). Two different networks were generated by IPA software, as reported in Figs. 6 and 7, corresponding to Pb(+2) and Cd(+2) exposure, respectively. For Pb(+2) treatment, the predicted top functions in which the listed proteins seem to be involved are cell death and cellular function and maintenance, with 17 proteins identified out of 35 proteins that form the predicted group with a total score of 46. The predicted effects illustrated by IPA for Cd exposure are related to cell death and development, involving 17 proteins out of 33 with a score of 49.

4 Discussion

Although essential in many cellular processes, metals become toxic when they are present in excess, as they induce severe impairment of cell functions. Cadmium is an important environmental pollutant that causes damage to various organs, especially to renal proximal tubular cells[19] and a well known carcinogen. Although exposure to high concentrations of lead is less common than in the past, lead pollution is still a cause of nephrotoxicity.

The effects of heavy metals have been studied in a variety of living cells and organisms, ranging from bacteria or fungi[20] to invertebrates[21], plants[22], mammalian cells[23,24,25] and animal models[26], with the ultimate goal of investigating tolerance mechanisms and identifying potential biomarkers for detecting heavy metal toxicity. It emerges that metals induce oxidative stress and apoptosis and that specific responses to metal exposure are elicited by different organisms.

In the present report, the effects of cadmium and lead on the viability of human primary renal cells (HRCE cell line) were investigated, as well as their impact on cell proteome. This cell line is particularly appropriate as a model system, as kidneys are the first target organs of heavy metals being able to reabsorb and accumulate divalent metals.

We showed that the viability of HRCE cells, exposed either to cadmium or lead, is severely impaired. The toxic effects are particularly evident with cadmium, as at a concentration as low as 10 μg/mL after 24 h about 50% of cells are strongly affected in their metabolic activity, whereas, at the same concentration of lead, about 30% of the exposed cells is impaired. Interestingly, in both cases the toxic effects are dose- and time-dependent.

Death is eventually caused by apoptosis, as demonstrated by the presence of Hoechst positive nuclei, often abnormal in shape. The analysis of the apoptotic pathway revealed an apparent activation of the caspase-9 associated pathway, a significant down-regulation of the anti-

apoptotic marker Bcl-2 with a consequent procaspase-3 cleavage (Fig. 3). In line with the data on the effects of heavy metals on cell viability, cadmium was found to be more toxic than lead in inducing apoptosis (Table 1). However, on the basis of the collected data, we hypothesize that, in the case of lead, the observed cell death is not exclusively due to apoptosis activation, as a modest decrease of procaspase-3 is observed compared to the extent of cell death induced by the metal. Hence, more than one mechanism could be activated by lead, so that further analyses will be performed to deeply inspect this phenomenon. Our results are in line with other *in vitro* studies on human cell lines[23,24] showing increased DNA fragmentation and caspase-3 activation upon heavy metals treatment, as well as with *in vivo* studies[26] demonstrating apoptotic cell death in proximal renal tubules of experimental animals following cadmium exposure.

We performed a systematic proteomic investigation of the effects of heavy metals on the proteome of cultured renal cells. More than three hundred protein spots were analyzed in search of significant variation in protein levels as a consequence of cell exposure to heavy metals. We found that 25 protein spots showed a significant difference in volume with respect to the corresponding spots of untreated cells. All the spots were analyzed by nanoLC-MS/MS and 27 proteins particularly affected in their expression levels by metal exposure were identified (Table 3). It is interesting to notice the down-regulation effect of cadmium on all the affected proteins, whereas a positive or negative effect on protein expression levels is elicited by lead.

The analysis of the functional role of differentially expressed proteins revealed that a significant number (48%) play a direct role in apoptotic cell death in the case of cadmium, whereas a slighter effect (18%) was observed for lead. On the other hand, 36% of the proteins affected by lead is involved in protein folding versus 19% observed after cadmium exposure (Fig. 5).

Although Cd is a well known tumorigenic agent, no proteins involved in carcinogenesis were observed. This is in line with the recent observation that to induce carcinogenesis in bronchial

epithelial cells, exposure to low Cd levels (up to 2 μM) over a prolonged period of time (2 months) is needed [27]. In our experimental system, instead, cells were transiently exposed to high Cd doses (100 μM, corresponding to the IC_{50} value) to investigate at a proteomic level differentially expressed proteins.

Pathway analysis using Ingenuity software clearly indicated that for both metals most of the affected proteins are included in the cellular network "cell death and cellular function and maintenance" (Figs. 6 and 7).

Among these, we found that PARK7 is down-regulated by cadmium treatment, while it is unaffected by lead. PARK7 is an anti-apoptotic agent, as it protects cells against oxidative stress and cell death, acting during apoptosis or autophagy phenomena. In response to oxidative stress, PARK7 translocates to the mitochondrion and then to the nucleus. Ren[28] reported that in PARK7 knockdown H1299 cells caspase-3 activation is accelerated and cell death is induced by UV exposure, suggesting that PARK7 protects cells against UVB-induced cell death, in association with mitochondrial Bcl-X_L.

It is well known that environmental changes, including metals and oxidative stress, cause alterations in the pattern of cellular stress protein expression. Among the proteins whose levels are affected by metal exposure, we identified proteins involved in protein folding. We found that PDIA3 and HSPA5 (also named GRP78), both acting in the endoplasmic reticulum (ER), were down-regulated following cadmium and lead exposure. Transitional endoplasmic reticulum ATPase (TER ATPase, also named VCP) was also found to be affected in the same way by both heavy metals. The functional role and subcellular localization of these proteins collectively indicate that heavy metal exposure of HRCE cells induce massive protein unfolding and ER stress by decreasing chaperone levels. To be connected to ER stress are also the decreased levels of HSPD1 and HSPA9 (also named GRP75), that contribute to protein folding within the ER.

In line with these results are those recently obtained in transiently exposed lung epithelial cells to 20 μM Cd, indicating that heat-shock proteins and antioxidative stress proteins are upregulated[29]. Moreover, cadmium has been reported to interfere with protein folding, leading to accumulation of misfolded proteins in ER[30] with an apparent different mechanism, in that a concomitant induction of heat shock protein GRP78 and ER stress response were observed in a renal epithelial cell line as a protection strategy against cadmium cytotoxicity.

Interestingly, we also identified proteins involved in the control and arrangement of the cytoscheleton. Tubulins and myosin appeared to be significantly decreased upon cadmium treatment. A possible explanation could be that cadmium binds to tubulin and myosin sulphydryl groups with a consequent decrease of the functional protein[31]. These proteins are instead up-regulated by lead.

Annexin A1 (ANXA1) levels were found to be increased by lead and decreased by cadmium. Annexins are eukaryotic multifunctional proteins that bind membranes in a calcium-dependent manner. It has been reported[32] that cadmium has a dual effect on annexin A1 expression in arterial endothelial cells, as it was up-regulated after 6 h of metal exposure and down-regulated after 24 h. In the same paper, Vimentin (VIM), which is part of the intermediate filaments, was also reported to be affected by cadmium treatment. Accordingly, our findings demonstrate a decrease of VIM upon treatment with both cadmium and lead.

Finally, proteins involved in cell metabolism are also affected by metal exposure. Enolase 1 (ENO1), the major glycolytic enolase in non-muscle and neuronal cells, was found to be increased upon lead exposure, being unaffected by cadmium. No alteration of ENO1 by cadmium was evidenced in urothelial cells by Aimola[25].

In conclusion, our results, obtained with a proteomic approach, provided an array of interconnecting signals activated in renal cells exposed to toxic heavy metals. The emerging

complex scenario reveals that the cellular protein pattern has been modified in response to metal exposure. A list of proteins whose levels appeared to be significantly altered was provided following their identification. Although the physiopathological conditions that occur *in vivo* when renal cells are exposed to poisonous agents can be hardly reproduced by an *in vitro* cell model, primary cells may represent a suitable choice. Therefore, the identified proteins might represent potential biomarkers for human renal cells exposure to cadmium or lead, making our study a contribution to the prediction of mammalian toxic responses to heavy metal environmental pollution.

5 Conclusions

Cadmium and lead are environmental pollutants, known to induce damage to various organs, especially to the kidneys. Using a primary human renal cell line as an experimental model, we demonstrated that $CdCl_2$ and $PbCl_2$ are responsible for time- and dose-dependent inhibition of cell viability, with cadmium the most effective as a toxic agent. Cell death is predominantly due to the activation of apoptosis, as indicated by classical apoptosis markers, such as condensed nuclei, SapK phosphorylation, procaspase-9 and -3 cleavage and Bcl-2 down-regulation.

A systematic analysis of the cell proteome before and after exposure to either heavy metals revealed that 27 proteins, out of more than 300, resulted to be significantly altered in their expression levels. Most of the proteins were affected by both metals, whereas some were influenced either by lead or cadmium. Classification of the identified proteins into functional groups provided an array of interconnecting pathways, predominantly involving apoptosis (about 50% in the case of cadmium), energetic metabolism and protein folding.

Acknowledgments

This work was supported by Programma Operativo Nazionale "Ricerca e Competitività 2007-2013" PON01_01802" and PON01_00117. We thank Dr. Francesco Itri for help in Western blot analyses.

The authors have declared no conflict of interest.

6 References

1 J. J. Wirth and R. S. Mijal, Adverse effects of low level heavy metal exposure on male reproductive function. *Syst Biol Reprod Med*. 2010, **56**, 147-167.

2 L. Järup, Hazards of heavy metal contamination. *Br Med Bull*. 2003, **68**, 167-182.

3 L. Ritter, K. Solomon, P. Sibley, K. Hall, P. Keen, G. Mattu, B. Linton, Sources, pathways, and relative risks of contaminants in surface water and groundwater: a perspective prepared for the Walkerton inquiry. *J Toxicol Environ Health A*. 2002, **65**, 1-142.

4 M. Monachese, J. P. Burton, G. Reid, Bioremediation and human tolerance to heavy metals through microbial processes: A potential role for probiotics? *Appl Environ Microbiol*. 2012, **78**, 6397-404.

5 M. Valko, H. Morris, M. T. Cronin, Metals, toxicity and oxidative stress. *Curr Med Chem*. 2005, 12, 1161-208.

6 K. Jomova, M. Valko, Redox cycling mechanisms in the colon. *Medical hypotheses* 2012, **79**, 418-419.

7 O. Barbier, G. Jacquillet, M. Tauc, M.Cougnon, P.Poujeol, Effect of heavy metals on, and handling by, the kidney. *Nephron Physiol*. 2005, **99**, 105-110.

8 W. P. Mao, J. L. Ye, Z. B. Guan, J. M. Zhao, C. Zhang, N. N. Zhang, P. Jiang, T. Tian, Cadmium induces apoptosis in human embryonic kidney [HEK] 293 cells by caspase-dependent and -independent pathways acting on mitochondria. *Toxicol In Vitro*. 2007, **21**, 343-354.

9 R. Shimoda, T. Nagamine, H. Takagi, M. Mori, M. P.Waalkes, Induction of apoptosis in cells by cadmium: quantitative negative correlation between basal or induced metallothionein concentration and apoptotic rate. *Toxicol Sci*. 2001, **64**, 208-215.

10 E. Sabath, M. L. Robles-Osorio, Renal health and the environment: heavy metal nephrotoxicity. *Nefrologia*. 2012, **32**, 279-286.

11 H. K. Jeon, H. S. Jin, D. H. Lee, W. S. Choi, C. K. Moon, Y. J. Oh, T. H. Lee, Proteome analysis associated with cadmium adaptation in U937 cells: identification of calbindin-D28k as a secondary cadmium-responsive protein that confers resistance to cadmium-induced apoptosis. *J Biol Chem*. 2004, **279**, 31575-31583.

12 E. Rousselet, A. Martelli, M. Chevallet, H. Diemer, A. Van Dorsselaer, T. Rabilloud, J. M. Moulis, Zinc adaptation and resistance to cadmium toxicity in mammalian cells: molecular insight by proteomic analysis. *Proteomics*. 2008, **8**, 2244-2255.

13 D. Wessel, U. I. Flügge, A method for the quantitative recovery of protein in dilute solution in the presence of detergents and lipids. *Anal Biochem*. 1984, **138**, 141-143.

14 U. K. Laemmli, Cleavage of structural proteins during the assembly of the head of bacteriophage T4. *Nature* 1970, **227**, 680-685.

15 D. F. Hochstrasser, A. Patchornik, C. R. Merril, Development of polyacrylamide gels that improve the separation of proteins and their detection by silver staining. *Anal Biochem*. 1988, **173**, 412-423.

16 A. Jiménez-Marín, M. Collado-Romero, M. Ramirez-Boo, C. Arce, J. J. Garrido, Biological pathway analysis by ArrayUnlock and Ingenuity Pathway Analysis. *BMC Proc*. 2009, **3**, S6.

17 C. Cecchi, A. Pensalfini, M. Stefani, S. Baglioni, C. Fiorillo, S. Cappadona, R. Caporale, D. Nosi, M. Ruggiero, G. Liguri, Replicating neuroblastoma cells in different cell cycle phases display different vulnerability to amyloid toxicity. *J. Mol. Med*. 2008, **86**, 197-209.

18 T. R. Downs, W. W. Wilfinger, Fluorometric quantification of DNA in cells and tissue. *Anal. Biochem*. 1983, **131**, 538-547.

19 P. L. Goering, M. P. Waalkes, C. D. Klaassen, Toxicology of cadmium. *Toxicology of Metals: Biochemical Aspects (Handbook of Experimental Pharmacology)* 1995, **115**, 189–214.

20 Cherrad, S., Girard, V., Dieryckx, C., Gonçalves, I. R., Dupuy, J. W., Bonneu, M., Rascle, C., Job, C., Job, D., Vacher, S., Poussereau, N., Proteomic analysis of proteins secreted by Botrytis cinerea in response to heavy metal toxicity. *Metallomics* 2012, *4*, 835-46.

21 P. R. Hunt, N. Olejnik, R. S. Robert, Toxicity ranking of heavy metals with screening method using adult Caenorhabditis elegans and propidium iodide replicates toxicity ranking in rat. *Food Chem Toxicol*. 2012, **50**, 3280-3290.

22 A. Kumar, M. N. Prasad, O. Sytar, Lead toxicity, defense strategies and associated indicative biomarkers in Talinum triangulare grown hydroponically. *Chemosphere* 2012, **89**, 1056-1065.

23 S. Nemmiche, D. Chabane-Sari, M. Kadri, P. Guiraud, Cadmium-induced apoptosis in the BJAB human B cell line: Involvement of PKC/ERK1/2/JNK signaling pathways in HO-1 expression. *Toxicology* 2012, **300**, 103-11.

24 M. E. Culbreth, J. A. Harrill, T. M. Freudenrich, W. R. Mundy, T. J. Shafer, Comparison of chemical-induced changes in proliferation and apoptosis in human and mouse neuroprogenitor cells. *Neurotoxicology* 2012, **33**, 1499-1510.

25 P. Aimola, M. Carmignani, A. R. Volpe, A. Di Benedetto, L. Claudio, M. P. Waalkes, A. Van Bokhoven, E. J. Tokar, P. P. Claudio, Cadmium induces p53-dependent apoptosis in human prostate epithelial cells. *PLoS One* 2012, **7**, e33647.

26 T. Hamada, A. Tanimoto, Y. Sasaguri, Apoptosis induced by cadmium. *Apoptosis* 1997, **2**, 359–367.

27 Y.O. Son, L. Wang, P. Poyil, A. Budhraja, J.A. Hitron, Z. Zhang, J.C. Lee, X. Shi, Cadmium induces carcinogenesis in BEAS-2B cells through ROS-dependent activation of PI3K/AKT/GSK-3β/β-catenin signaling. *Toxicol Appl Pharmacol.* 2012, **264**, 153-160.

28 H. Ren, K. Fu, D. Wang, C. Mu, G. Wang, Oxidized DJ-1 interacts with the mitochondrial protein BCL-XL. *J Biol Chem.* 2011, **286**, 35308-35317.

29 Y.M. Xu, Y. Zhou, D.J. Chen, D.Y. Huang, J.F. Chiu, A.T.Y. Lau, Proteomic analysis of cadmium exposure in cultured lung epithelial cells: evidence for oxidative stress-induced cytotoxicity. *Toxicol Res*. 2013, **2**, 280-287.

30 F. Liu, K. Inageda, G. Nishitai, M. Matsuoka, Cadmium induces the expression of Grp78, an endoplasmic reticulum molecular chaperone, in LLC-PK1 renal epithelial cells. *Environ. Health Perspect*. 2006, **114**, 859–864.

31 Z. Hertelendi, A. Tóth, A. Borbély, Z. Galajda, J. van der Velden, G. J. Stienen, I. Edes, Z. Papp, Oxidation of myofilament protein sulfhydryl groups reduces the contractile force and its Ca2+ sensitivity in human cardiomyocytes. *Antioxid Redox Signal*. 2008, **10**, 1175-1184.

32 D. Bernhard, A. Rossmann, B. Henderson, M. Kind, A. Seubert, G.Wick, Increased serum cadmium and strontium levels in young smokers: effects on arterial endothelial cell gene transcription. *Arterioscler Thromb Vasc Biol*. 2006, **26**, 833-838.

Figure legends

Figure 1: Dose-response curves upon treatment of HRCE cells with $CdCl_2$ (A) or $PbCl_2$ (B) for 24 h. Cell viability was expressed as the percentage of MTT reduction with respect to control cells, tested under the same conditions but in the absence of metal. (C) Time-course of the effects of $CdCl_2$ (10 µg/mL) and $PbCl_2$ (100 µg/mL) on the viability of HRCE cells determined by MTT assay for different lengths of time in the range 2-72 h. Error bars correspond to the s.d. values of three independent experiments. *P* values < 0.01.

Figure 2: Hoechst staining of HRCE cells untreated or treated with: 10 µg/mL puromycin for 4 h, 10 µg/mL $CdCl_2$, 100 µg/mL $PbCl_2$ for 24 and 48 h. All images were acquired at the same magnification. Arrows indicate apoptotic nuclei.

Figure 3: Analysis of apoptotic markers in HRCE cells untreated or treated with $CdCl_2$ (10 µg/mL) or $PbCl_2$ (100 µg/mL) for 24 h (A) and 48 h (B). Lane 1, cell lysate of untreated cells; lane 2, lysate of cells treated with $PbCl_2$; lane 3, lysate of cells treated with $CdCl_2$. Western blots were performed using antibodies directed towards procaspase-3, procaspase-9, Bcl-2 and phospho-SapK. Endogenous GAPDH (A) and alpha-actin (B) were used as internal standards.

Figure 4: Protein 2D maps of HRCE cells grown in control (A) and stimulated conditions (100 µg/mL $PbCl_2$ and 10 µg/mL $CdCl_2$ for B and C, respectively) in the acidic (4–7) pI range. Numbers and circles indicate differentially expressed protein spots submitted to proteomic analyses.

Figure 5: Schematic representation of multiple cellular processes in which the identified proteins are involved.

Figure 6: Canonical pathways identified by Ingenuity Pathway Analysis performed on differentially expressed proteins generated from 2D-GE nanoLC-MS/MS analysis after 24 h exposure to 100 µg/mL $PbCl_2$. Solid lines indicate direct interactions, dashed lines indicate

indirect interactions. Arrows indicate activation, bars inhibition. Squares indicate proteins identified by nanoLC-MS/MS.

Figure 7: Canonical pathways identified by Ingenuity Pathway Analysis performed on differentially expressed proteins generated from 2D-GE nanoLC-MS/MS analysis after 24 h exposure to 10 µg/mL $CdCl_2$. Solid lines indicate direct interactions, dashed lines indicate indirect interactions. Arrows indicate activation, bars inhibition. Squares indicate proteins identified by nanoLC-MS/MS.

Table 1: Quantitative analysis of apoptotic marker levels (SapK, procaspase-9, procaspase-3 and Bcl-2) in HRCE cells untreated or treated with $PbCl_2$ (100 µg/mL) or $CdCl_2$ (10 µg/mL) for 24 h (A) and 48 h (B). For each sample, the protein intensity level was normalized to endogenous GAPDH (A) or alpha-actin (B) and compared to that of untreated cells. The data represent the means ± standard deviation of protein levels determined in three independent experiments.

A

Sample	SapK (%)	Procaspase-9 (%)	Procaspase-3 (%)
Untreated cells	100	100	100
Cells treated with $PbCl_2$	108 ± 6	86 ± 10	100 ± 5
Cells treated with $CdCl_2$	972 ± 3	33 ± 8	100 ± 4

B

Sample	Procaspase-3 (%)	Bcl-2 (%)
Untreated cells	100	100
Cells treated with $PbCl_2$	68 ± 5	77 ± 6
Cells treated with $CdCl_2$	45 ± 4	47 ± 3

Table 2: Quantitative ICP-MS analysis of HRCE cells treated with $PbCl_2$ (100 µg/mL) or $CdCl_2$ (10 µg/mL) for 24 h. Quantifications were obtained in triplicate. Intracellular metal concentrations were normalized to the total protein content.

Sample	**Pb(+2) (%)**	**Cd(+2) (%)**
Total amount	100 ± 0.6	100 ± 4.5
Cell conditioned medium	92.7 ± 2.6	88.9 ± 0.4
Cell washing	6.5 ± 2,1	9.6 ± 2.4
Cell lysate	0.691 ± 0.006	0.276 ± 0.002

Table 3: List of the proteins identified by nanoLC-MS/MS. Spot numbers refer to Fig. 4. Variation in fold expression are given by the comparison of each spot with the control. +/- indicates increment/decrement with respect to the control; =, no change in the expression level; ud, undetectable spot in the 2D maps. MW, Score, Number of peptides, Peptide sequences and Sequence coverage are reported in supplementary material (Table S1).

No. protein spots	Protein Code	Protein Name	UniProt accession	Fold change after $PbCl_2$ treatment	Fold change after $CdCl_2$ treatment
1	PARK7	Protein DJ-1	Q99497	=	- 0,4
2	EF1D	Elongation Factor 1-Delta	P29692	- 0,6	ud
3	TUBB	Tubulin Beta Chain	P07437	+ 0,7	ud
4	MLC-3	Myosin Light Polypeptide 6	P60660	+ 2,5	ud
5	S100A11	Protein S100-A11	P31949	+ 0,3	- 0,4
6	VCP	Transitional Endoplasmic Reticulum ATPase	P55072	- 0,7	- 0,8
7	CALD1	Caldesmon	Q05682	- 0,7	- 0,6
8	HSPA9	Stress-70 Protein, Mitochondrial	P38646	- 0,7	=
9	CCT5	T-complex Protein 1 Subunit Epsilon	P48643	- 0,7	- 0,3
	HSPD1	60kDa Heat Shock Protein, Mitochondrial	P10809	- 0,7	- 0,3
10	HSPA5	78 kDa Glucose-regulated protein	P11021	- 0,7	- 0,5
11	LYS	Lysozyme C	P61626	- 0,8	- 0,6
12	CCT2	T-complex Protein 1 Subunit Beta	P78371	- 0,6	- 0,7
13	ENO1	Alpha-Enolase	P06733	+ 0,3	=
14	EF1B	Elongation Factor 1-Beta	P24534	+ 0,6	- 0,8
15	DDAH-2	N[G], N[G]-Dimethylarginine Dimethylaminohydrolase 2	O95865	+ 2,5	- 0,5
16	ANXA1	Annexin A1	P04083	+ 0,5	- 0,3

17	TPI1	Triosephosphate Isomerase	P60174	=	- 0,6
18	HSPB1	Heat Shock Protein Beta-1	P04792	+ 0,6	=
19	NME1	Nucleoside Diphosphate Kinase A	P15531	=	- 0,6
20	UCH-L1	Ubiquitin Carboxyl-terminal hydrolase isozyme L1	P09936	=	0,5
21	TUBB2C	Tubulin Beta-4B Chain	P68371	+ 1,1	ud
22	VIM	Vimentin	P08670	- 0,4	- 0,4
23	PDIA3	Protein Disulfide-Isomerase A3	P30101	- 0,5	- 0,5
24	LGALS1	Galectin-1	P09382	=	- 0,5
25	PP17	Perilipin-3	O60664	- 0,6	=
	ACTB	Actin, Cytoplasmic	P60709	- 0,6	=

Cadmium and lead affect viability of primary human renal cells, inducing alterations of cellular proteome

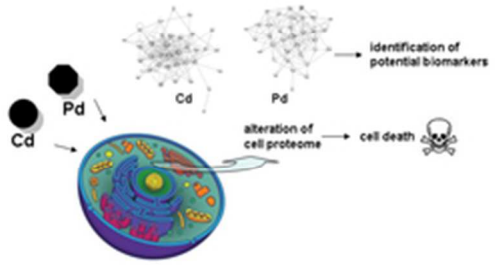

30x22mm (300 x 300 DPI)

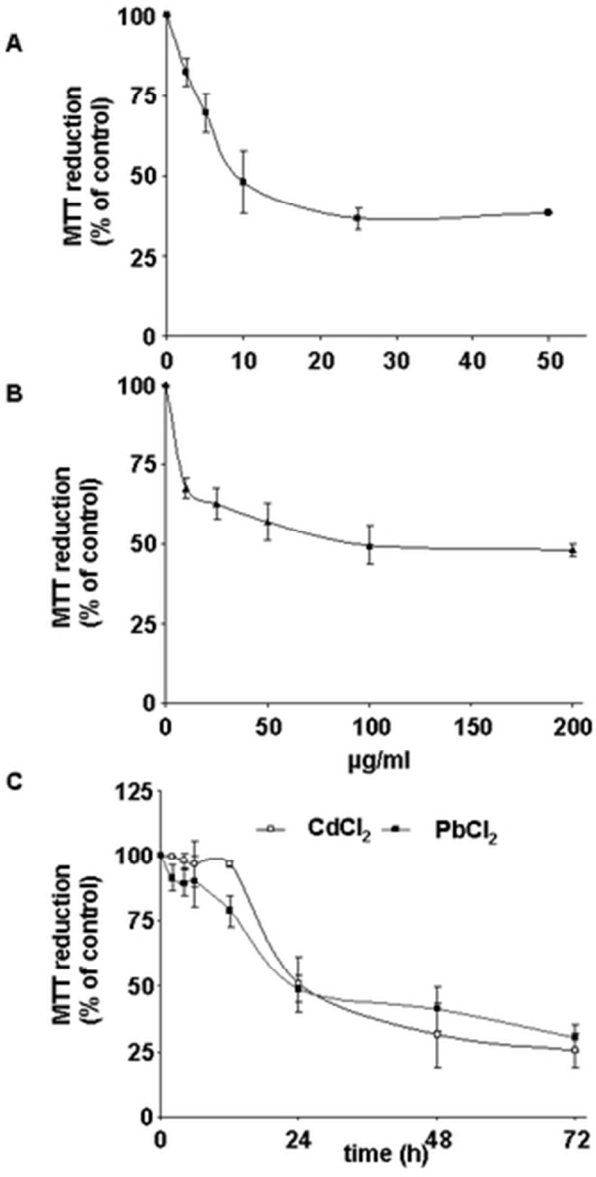

40x54mm (300 x 300 DPI)

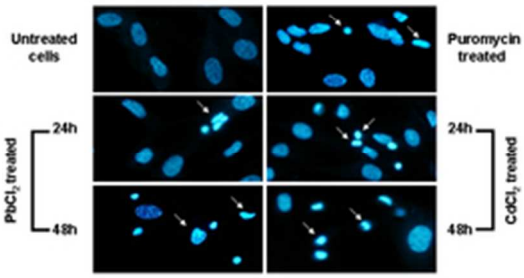

30x22mm (300 x 300 DPI)

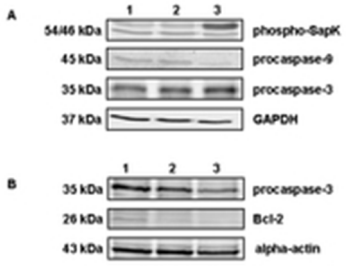

18x12mm (300 x 300 DPI)

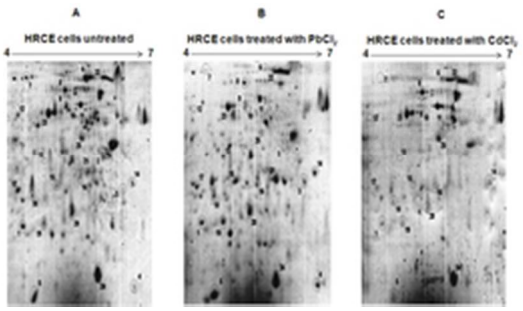

22x12mm (300 x 300 DPI)

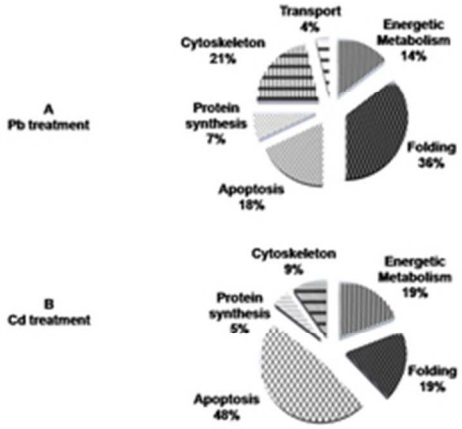

28x20mm (300 x 300 DPI)

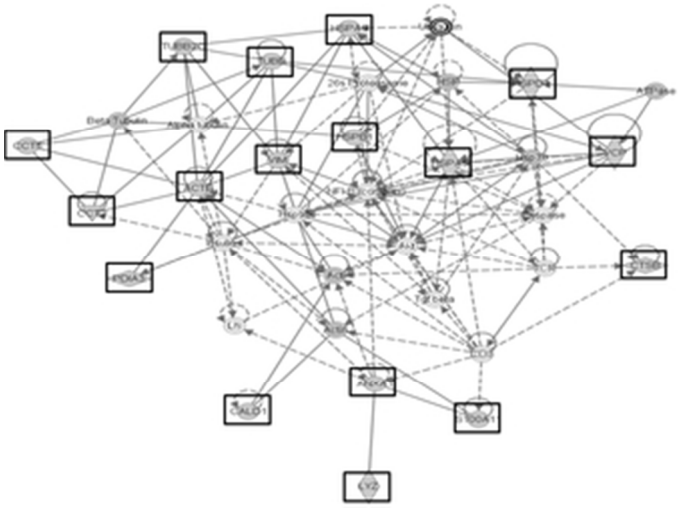

28x21mm (300 x 300 DPI)

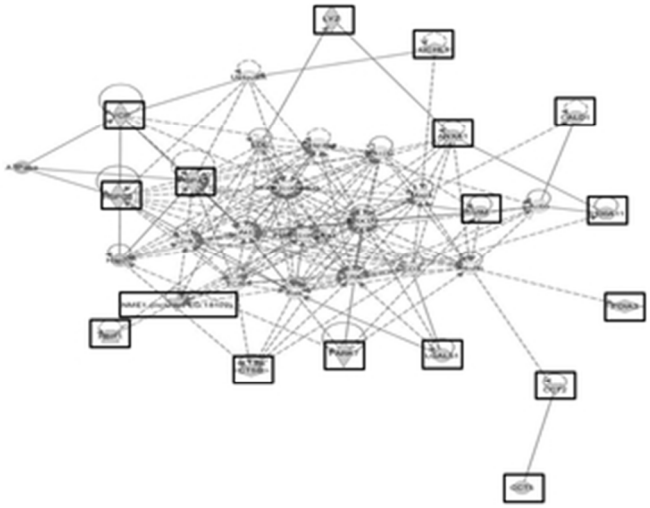

28x21mm (300 x 300 DPI)

Supplementary data (Table S1)

Spot	MW	Total Score	Protein	ID Swissprot	N. of peptides	Peptide Sequence	Precursor ion (m/z)	Peptide Charge	Modification	Sequence coverage (%)	pI Theor.
1	20050	187	Protein DJ-1	Q99497	8	K.APLVLKD.- (27)	378.23	2+		30	6.33
						K.VTTHPLAK.D (22)	433.76	2+			
						K.VTVAGLAGKDPVQCSR.D (32)	553.29	3+			
						K.GAEEMETVIPVDVMR.R (23)	838.41	2+			
						K.GAEEMETVIPVDVMRR.R (19)	611.3	3+			
						R.AGIKVTVAGLAGKDPVQCSR.D (23)	676.37	3+			
						R.ALVILAKGAEEMETVIPVDVMR.R (22)	806.1	3+	2 M(ox)		
						R.ALVILAKGAEEMETVIPVDVMRR.R (19)	858.13	3+	2 M(ox)		
2	31217	107	Elongation Factor 1-Delta	P29692	4	K.KPALVAK.S (26)	363.75	2+		14	4.90
						K.LVPVGYGIR.K (21)	487.3	2+			
						R.SIQLDGLVWGASK.L (44)	687.37	2+			
						R.ATAPQTQHVSPMR.Q (16)	475.25	3+			
3	50095	132	Tubulin Beta Chain	P07437	4	R.IMNTFSVVPSPK.V (35)	668.36	2+	M(ox)	18	4.78
						R.AILVDLEPGTMDSVR.S (34)	816.42	2+	M(ox)		
						R.ISVYYNEATGGKYVPR.A (24)	606.32	3+			
						R.SGPFGQIFRPDNFVFGQSGAGNNWAK.G (39)	933.46	3+			
4	17090	205	Myosin Light Polypeptide 6	P60660	7	K.SDEMNVK.V (33)	411.69	2+		41	4.56
						R.HVLVTLGEK.M (22)	498.30	2+			
						K.ILYSQCGDVMR.A (33)	671.32	2+			
						R.ALGQNPTNAEVLK.V (49)	677.88	2+			
						K.VLGNPKSDEMNVK.V (28)	477.59	3+			
						K.VLDFEHFLPMLQTVAK.N (22)	635.34	3+	M(ox)		
						R.ALGQNPTNAEVLKVLGNPK.S (18)	655.04	3+			
5	11847	196	Protein S100-A11	P31949	5	K.DPGVLDR.M (42)	386.20	2+		60	6.56
						K.ISSPTETER.C (36)	510.26	2+			
						K.DGYNYTLSK.T (42)	530.75	2+			
						K.TEFLSFMNTELAAFTK.N (60)	933.45	2+	M(ox)		
						K.ISSPTETERCIESLIAVFQK.Y (16)	770.07	3+			

6	89950	179	Transitional Endoplasmic Reticulum ATPase	P55072	7	K.FGMTPSK.G (22)	384.19	2+		16	5.14
						R.KGDIFLVR.G (38)	474.29	2+			
						K.LAGESESNLR.K (18)	538.28	2+			
						R.GGNIGDGGGAADR.V (32)	558.76	2+			
						R.IVSQLLTLMDGLKQR.A (26)	577.67	3+	M(ox)		
						R.QAAPCVLFFDELDSIAK.A (22)	962.48	2+			
						R.ETVVEVPQVTWEDIGGLEDVKR.E (21)	833.42	3+			
7	93232	78	Caldesmon	Q05682	3	R.LQEALER.Q (17)	429.74	2+		7	5.62
						R.LEQYTSAIEGTK.S (35)	670.34	2+			
						R.QKEFDPTITDASLSLPSRR.M (28)	715.37	3+	(N-term		
8	73920	962	Stress-70 Protein, Mitochondrial	P38646	25	R.NTTIPTK.K (24)	387.72	2+		46	5.87
						K.YAEEDR.R (20)	391.68	2+			
						R.TIAPCQK.A (26)	409.21	2+			
						R.ETGVDLTK.D (23)	431.73	2+			
						R.NTTIPTKK.S (20)	451.77	2+			
						K.VLENAEGAR.T (50)	479.75	2+			
						K.DSETGENIR.Q (17)	510.74	2+			
						R.QAASSLQQASLK.L (41)	616.34	2+			
						K.DAGQISGLNVLR.V (49)	621.86	2+			
						K.VQQTVQDLFGR.A (53)	645.85	2+			
						R.YDDPEVQKDIK.N (33)	675.33	2+			
						R.AQFEGIVTDLIR.R (35)	681.37	2+			
						K.NAEKYAEEDRR.K (17)	460.89	3+			
						R.AQFEGIVTDLIRR.T (26)	506.62	3+			
						K.LYSPSQIGAFVLMK.M (44)	777.42	2+			
						R.QAVTNPNNTFYATK.R (45)	784.89	2+			
						K.LLGQFTLIGIPPAPR.G (29)	796.98	2+			
						R.VINEPTAAALAYGLDK.S (79)	823.45	2+			
						K.VQQTVQDLFGRAPSK.A (22)	558.64	3+			
						R.ETGVDLTKDNMALQR.V (38)	564.29	3+			
						K.NAVITVPAYFNDSQR.Q (54)	847.93	2+			
						R.QAVTNPNNTFYATKR.L (32)	575.64	3+			
						K.SQVFSTAADGQTQVEIK.V (88)	904.96	2+			
						R.EMAGDNKLLGQFTLIGIPPAPR.G (25)	785.42	3+	M(ox)		
						K.AMQDAEVSKSDIGEVILVGGMTR.M (72)	808.07	3+	M(ox)		

9	60089	178	T-complex Protein 1 Subunit Epsilon	P48643	7	K.AVANTMR.T (19)	381.70	2+		22	5.45
						R.AVTIFIR.G (24)	410.26	2+			
						R.TSLGPNGLDK.M (22)	501.27	2+			
						K.MLVIEQCK.N (15)	510.77	2+			
						R.IADGYEQAAR.V (43)	547.28	2+			
						R.SLHDALCVIR.N (15)	395.22	2+			
						K.IAILTCPFEPPKPK.T (40)	537.64	3+			
	61187	133	60kDa Heat Shock Protein, Mitochondria l	P10809	4	K.LSDGVAVLK.V (24)	451.27	2+		11	5.70
						R.VTDALNATR.A (22)	480.76	2+			
						K.NAGVEGSLIVEK.I (32)	608.32	2+			
						R.AAVEEGIVLGGGCALLR.C (55)	842.96	2+			
10	72402	90	78 kDa Glucose-regulated protein	P11021	3	R.TWNDPSVQQDIK.F (25)	715.86	2+		4	5.07
						K.NQLTSNPENTVFDAK.R (19)	839.40	2+			
						K.NQLTSNPENTVFDAKR.L (46)	611.97	3+			
11	16982	116	Lysozyme C	P61626	4	R.LGMDGYR.G (16)	406.19	2+		24	9.38
						R.ATNYNAGDR.S (48)	491.22	2+			
						K.WESGYNTR.A (16)	506.73	2+			
						R.STDYGIFQINSR.Y (36)	700.84	2+			
12	57794	88	T-complex Protein 1 Subunit Beta	P78371	4	K.IGVNQPK.R (18)	378.23	2+		8	6.01
						K.VLVDMSR.V (30)	410.23	2+			
						R.VRVDSTAK.V (25)	438.25	2+			
						K.RIENAK.I (15)	365.72	2+			
13	47481	67	Alpha-Enolase	P06733	3	K.AVEHINK.T (15)	405.73	2+		5	7.01
						R.IAKAVNEK.S (26)	436.76	2+			
						K.TIAPALVSK.K (26)	450.28	2+			
14	24919	176	Elongation Factor 1-Beta	P24534	6	K.KPALVAK.S (21)	363.75	2+		20	4.50
						K.ASLPGVKK.A (15)	400.26	2+			
						R.LAQYESK.K (30)	419.72	2+			
						K.LVPVGYGIK.K (26)	473.29	2+			
						R.LAQYESKK.A (18)	483.77	2+			
						R.SIQADGLVWGSSK.L (66)	674.35	2+			

15	29911	150	N(G), N(G)-Dimethylarginine Dimethylaminohydrolase 2	O95865	5	K.ALQDLGLR.I (35)	443.26	2+		24	5.66
						R.GLCGMGGPR.T (18)	452.71	2+			
						R.GGGDLPNSQEALQK.L (28)	707.35	2+			
						R.TVVAGSSDAAQKAVR.A (46)	487.27	3+			
						R.GVPESLASGEGAGAGLPALDLAK.A (23)	1040.55	2+			
16	38918	76	Annexin A1	P04083	3	R.SYPQLR.R (16)	382.21	2+		8	6.57
						R.ALYEAGER.R (34)	454.73	2+			
						K.GTDVNVFNTILTTR.S (26)	775.90	2+			
17	31057	262	Triosephosphate Isomerase	P60174	9	R.QKLDPK.I (16)	356.21	2+	Pyro-glu (N-term Q)	33	5.65
						K.VVFEQTK.V (17)	425.74	2+			
						K.IAVAAQNCYK.V (29)	569.29	2+			
						K.SNVSDAVAQSTR.I (58)	617.81	2+			
						K.VIADNVKDWSK.V (16)	425.56	3+			
						K.TATPQQAQEVHEK.L (23)	489.58	3+			
						K.VVLAYEPVWAIGTGK.T (36)	801.94	2+			
						R.QKLDPKIAVAAQNCYK.V (21)	610.66	3+	Pyro-glu (N-term Q)		
						K.VPADTEVVCAPPTAYIDFAR.Q (46)	1096.53	2+			
18	22826	114	Heat Shock Protein Beta-1	P04792	3	R.LFDQAFGLPR.L (44)	582.31	2+		21	5.95
						R.AQLGGPEAAKSDETAAK.- (39)	548.61	3+			
						K.LATQSNEITIPVTFESR.A (31)	953.49	2+			
19	17309	107	Nucleoside Diphosphate Kinase A	P15531	4	R.GDFCIQVGR.N (33)	526.26	2+		43	5.83
						R.TFIAIKPDGVQR.G (28)	448.93	3+			
						R.VMLGETNPADSKPGTIR.G (29)	601.31	3+	M(ox)		
						K.YMHSGPVVAMVWEGLNVVK.T (17)	716.69	3+	2 M(ox)		

20	25151	352	Ubiquitin Carboxyl-terminal hydrolase isozyme L1	P09936	11	R.EQGEVR.F (20)	359.18	2+		82	5.33
						K.MSPEDR.A (31)	367.66	2+			
						K.QIEELK.G (20)	380.22	2+			
						R.LGVAGQWR.F (29)	443.75	2+			
						R.FSAVALCK.A (42)	448.24	2+			
						K.QFLSETEK.M (27)	491.25	2+			
						R.FSAVALCKAA.- (38)	519.28	2+			
						R.EFTEREQGEVR.F (15)	460.56	3+			
						K.QIEELKGQEVSPK.V (41)	742.91	2+			
						K.NEAIQAAHDAVAQEGQCR.V (42)	656.64	3+			
						K.QTIGNSCGTIGLIHAVANNQDKLGFEDGSVLK	1113.89	3+	(N-term Q)		
21	50255	113	Tubulin Beta-4B Chain	P68371	3	K.LAVNMVPFPR.L (41)	580.33	2+	M(ox)	10	4.79
						R.IMNTFSVVPSPK.V (31)	668.36	2+	M(ox)		
						R.AVLVDLEPGTMDSVR.S (41)	801.41	3+			
22	53676	402	Vimentin	P08670	14	R.SSVPGVR.L (45)	351.21	2+		46	5.06
						R.FLEQQNK.I (29)	453.74	2+			
						K.LLEGEESR.I (30)	466.74	2+			
						R.LRSSVPGVR.L (15)	485.79	2+			
						R.QQYESVAAK.N (41)	512.26	2+			
						R.TLLIKTVETR.D (22)	391.92	3+			
						R.QVDQLTNDKAR.V (31)	644.34	2+			
						R.SLYASSPGGVYATR.S (37)	714.86	2+			
						K.ILLAELEQLKGQGK.S (16)	513.98	3+			
						R.ISLPLPNFSSLNLR.E (28)	785.95	2+			
						R.LGDLYEEEMRELR.R (15)	551.60	3+			
						R.VEVERDNLAEDIMR.L (20)	563.61	3+			
						R.ETNLDSLPLVDTHSKR.T (31)	608.99	3+			
						R.QVQSLTCEVDALKGTNESLER.Q (42)	793.06	3+			

23	57146	1230	Protein Disulfide-Isomerase A3	P30101	39	K.KYEGGR.E (25)	355.19	2+		62	5.98
						R.VMMVAK.K (15)	355.68	2+	2 M(ox)		
						R.DGKALER.F (17)	394.72	2+			
						R.VMMVAKK.F (18)	411.73	2+	M(ox)		
						K.KKAQEDL.- (15)	416.23	2+			
						K.YKELGEK.L (17)	433.74	2+			
						K.DPNIVIAK.M (19)	435.26	2+			
						K.LNFAVASR.K (40)	439.25	2+			
						R.LKGIVPLAK.V (28)	469.82	2+			
						K.TVAYTEQK.M (24)	470.24	2+			
						R.NRVMMVAK.K (25)	482.76	2+	M(ox)		
						K.YGVSGYPTLK.I (42)	542.79	2+			
						R.TADGIVSHLKK.Q (18)	390.23	3+			
						R.LAPEYEAAATR.L (43)	596.30	2+			
						K.LSKDPNIVIAK. (47)	399.91	3+			
						R.DGEEAGAYDGPR.T (42)	618.76	2+			
						R.GFPTIYFSPANK.K (45)	671.35	2+			
						K.RLAPEYEAAATR.L (26)	449.91	3+			
						K.SEPIPESNDGPVK.V (25)	684.84	2+			
						R.ELSDFISYLQR.E (48)	685.85	2+			
						K.VDCTANTNTCNK.Y (61)	699.29	2+			
						R.LAPEYEAAATRLK.G (32)	478.27	3+			
						R.GFPTIYFSPANKK.L (22)	490.60	3+			
						K.FVMQEEFSRDGK.A (20)	496.90	3+	M(ox)		
						K.YGVSGYPTLKIFR.D (25)	500.95	3+			
						R.FLQDYFDGNLKR.Y (37)	758.38	2+			
						R.EATNPPVIQEEKPK.K (30)	790.42	2+			
						K.DLLIAYYDVDYEK.N (52)	810.40	2+			
						K.FLDAGHKLNFAVASR.K (41)	549.30	2+			
						K.IFRDGEEAGAYDGPR.T (22)	551.60	3+			
						K.MDATANDVPSPYEVR.G (69)	832.89	2+			
						R.TAKGEKFVMQEEFSR.D (18)	596.30	3+			
						K.QAGPASVPLRTEEEFKK.F (23)	624.00	3+	Pyro-glu (N-term Q)		
						K.DLLIAYYDVDYEKNAK.G (29)	644.99	2+			
						R.LKGIVPLAKVDCTANTNTCNK.Y (25)	773.08	3+			
						K.TFSHELSDFGLESTAGEIPVVAIR.T (62)	859.11	3+			
						R.KTFSHELSDFGLESTAGEIPVVAIR.T (47)	901.80	3+			
						K.LSKDPNIVIAKMDATANDVPSPYEVR.G (36)	715.62	3+	M(ox)		

24	15048	720	Galectin-1	P09382	15	R.GEVAPDAK.S (23)	393.70	2+		85	5.34
						K.IKCVAFD.- (17)	426.72	2+			
						K.SFVLNLGK.D (57)	439.26	2+			
						K.LPDGYEFK.F (23)	484.74	2+			
						K.DGGAWGTEQR.E (67)	538.74	2+			
						K.LPDGYEFKFPNR.L (52)	741.87	2+			
						K.DSNNLCLHFNPR.F (51)	743.85	2+			
						R.FNAHGDANTIVCNSK.D (43)	824.39	2+			
						R.LNLEAINYMAADGDFK.I (77)	892.93	2+			
						R.VRGEVAPDAKSFVLNLGK.D (33)	634.03	3+			
						R.LNLEAINYMAADGDFKIK.C (67)	1013.51	2+			
						K.FPNRLNLEAINYMAADGDFK.I (44)	767.04	3+			
						K.SFVLNLGKDSNNLCLHFNPR.F (40)	782.40	3+			
						R.EAVFPFQPGSVAEVCITFDQANLTVK.L (84)	956.48	3+	M(ox)		
						K.DSNNLCLHFNPRFNAHGDANTIVCNSK.D (42)	1039.14	3+			
25	47217	273	Perilipin-3	O60664	7	R.LGSLSER.L (21)	381.21	2+		25	5.30
						R.QEQSYFVR.L (35)	528.76	2+			
						K.TVCDAAEKGVR.T (23)	402.54	3+			
						K.SVVTGGVQSVMGSR.L (54)	682.36	2+			
						R.TLTAAAVSGAQPILSK.L (61)	764.44	2+			
						R.QVEDLQATFSSIHSFQDLSSSILAQSR.E (35)	993.15	3+	Pyro-glu (N-term Q)		
						R.TLTAAAVSGAQPILSKLEPQIASASEYAHR.G (4	1027.54	3+			
	42052	214	Actin, Cytoplasmic	P60709	6	K.IIAPPER.K (27)	398.24	2+		37	5.29
						K.AGFAGDDAPR.A (64)	488.73	2+			
						R.GYSFTTTAER.E (15)	566.77	2+			
						K.EITALAPSTMK.I (33)	581.32	2+			
						K.SYELPDGQVITIGNER.F (55)	895.95	2+			
						R.VAPEEHPVLLTEAPLNPK.A (20)	652.03	3+			